NMR free ligand conformations and atomic resolution dynamics

Amber Y.S. Balazs[1], Nichola L. Davies[2], David Longmire[2], Martin J. Packer[2], Elisabetta Chiarparin[2]

[1]Chemistry, Oncology R&D, AstraZeneca, Waltham, Massachusetts 02451, United States
[2]Chemistry, Oncology R&D, AstraZeneca, Cambridge CB4 0QA, United Kingdom

5 *Correspondence to*: Amber Y.S. Balazs (amber.balazs@astrazeneca.com)

Abstract. Knowledge of free ligand conformational preferences (energy minima) and conformational dynamics (rotational energy barriers) of small molecules in solution can guide drug design hypotheses and help rank ideas to bias syntheses towards more active compounds. Visualization of conformational exchange dynamics around torsion angles, by replica-exchange with solute tempering molecular dynamics (REST-MD), gives results in agreement with high resolution ^1H NMR
10 spectra and complements free ligand conformational analyses. Rotational energy barriers around individual bonds are comparable between calculated and experimental values, making the in silico method relevant to ranking prospective design ideas in drug discovery programs, particularly across a series of analogues. Prioritizing design ideas, based on calculations and analysis of measurements across a series, efficiently guides rational discovery towards the 'right molecules' for effective medicines.

1 Introduction

NMR signal line shapes inherently provide atomic-level, site-specific insights into structural dynamics. High resolution ^1H NMR signals broaden when small molecules in solution undergo exchange dynamics on a millisecond timescale. In contrast, sharp NMR resonance signals may indicate either a dominant pre-organized conformation or an ensemble of flexible molecules undergoing fast equilibrium exchange between rotational isomers. Comparisons between experimental and
20 computed NMR parameter values (shifts, NOEs, *J*-couplings) can identify relative populations of conformers, such as a singular, highly populated conformation, with well defined internuclear distances and torsion angles or an averaged solution structure, composed of multiple conformations, each at a low molar fraction of the total, resulting from low barriers to rotation around bonds. NMR analysis of molecular flexibility in solution (NAMFIS; Cicero et al., 1995) takes the approach of systematically varying percent contributions from sets of conformers generated in silico, together with the corresponding
25 *calculated* NMR parameter values, compared against the experimental data. The sum of square differences determines the goodness-of-fit between experimental and calculated values to select a best-fit population weighted model. The fundamental concept of filtering theoretical conformations through experimental data to derive the best fit has become well established over the decades, together with variations in details of implementation, to determine the conformational preference(s) of a small molecule in solution (Cicero et al., 1995; Nevins et al, 1999; Slabber et al., 2016; Wu et al., 2017; Balazs et al., 2019;
30 Farès et al., 2019; Atilaw et al., 2021).

Determining the conformational profile of a free ligand in solution enhances early drug discovery programs (LaPlante et al., 2014; Blundell et al., 2016; Foloppe and Chen, 2016; Chiarparin et al., 2019). A general overview of how NMR fits into Medicinal Chemistry design cycles is illustrated in Fig. 1. An efficacious pharmaceutical that positively impacts patients' lives starts with Medicinal Chemistry teams designing the right molecule. Design teams need to understand whether a molecule readily adopts its "bioactive" conformation in solution to optimize the binding on-rate through reduced conformational entropy and energetic penalty paid on conformational rearrangement to the proper binding mode. In addition, pre-organization of the free ligand in solution would indicate minimized conformational strain energy in the bound molecule. If not, the challenge is to conceive of ideas to modify the structure to discover a new molecule to favor this conformation. Towards this aim of optimizing the free energy of binding, it is desirable for ligands in solution to preferentially pre-organize into the bioactive binding mode (Blundell et al., 2013; Balazs et al., 2019). Molecular rigidification strategies (Fang et al., 2014; de Sena M Pinheiro et al., 2019) increase pre-organization and NMR conformational analysis can deconvolute and report on the molar fraction adopting the bioactive conformation. Structure based drug design (SBDD) can be enhanced by ready access to 3D free ligand average solution conformations to complement X-ray crystallographic models of the bound ligand and protein-ligand interactions (Blundell et al., 2013; Chiarparin et al., 2019; Balazs et al., 2019). Faster design cycles require quick turnover times in analyzing solution conformations of synthesized compounds. Design cycles can be accelerated through faster computational schemes, efficient automation to obtain NMR spectral parameters, and recognition of conformational signatures from 1D NMR spectra (Balazs et al., 2019), also named, "SAR by 1D NMR" (Zondlo, 2019).
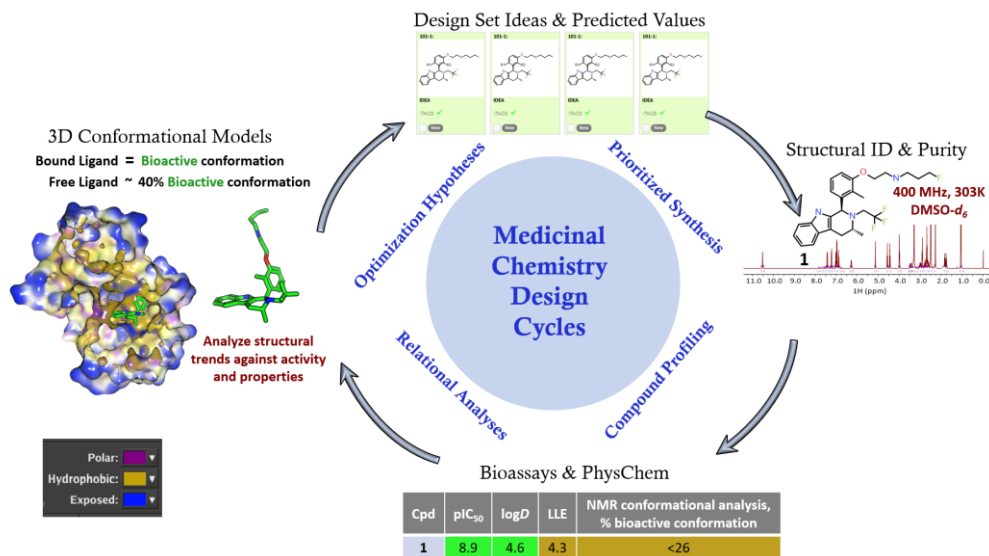
Figure 1. An illustrative Medicinal Chemistry design cycle for drug discovery with inhibition (pIC$_{50}$) and the octanol/water partition coefficient (log$D$) values from a recent Oncology R&D project (Scott et al., 2016; Scott et al., 2019; Scott et al., 2020). NMR plays a key role in synthesis support for structural identification and analysis of compound purity. NMR also can be used to enhance structure based drug design through NMR free ligand conformational analysis. This provides the relative population of the bioactive conformation in solution by determining the percentages of the minimal energy conformers. Structure based drug design is enhanced through measured extent of free-ligand pre-organization into the bioactive conformation, which lends itself to rigidification design hypotheses aimed at optimized binding to the protein target.

Herein, we demonstrate incorporation of molecular dynamics, specifically an efficient version using replica-exchange with solute tempering (REST-MD) (Liu et al., 2005; Huang et al., 2007; Wang et al., 2011), into an NMR based semi-automatic drug discovery platform, to visualize rotational barriers around molecular bonds. Good agreement is demonstrated between REST-MD calculated energy barriers and NMR measurements, using a small molecule selective estrogen-receptor degrader (SERD) example from a recent Oncology R&D project (Scott et al., 2016; Scott et al., 2019; Scott et al., 2020). The theoretical and experimental data complement each other: REST-MD simplifies the interpretation of NMR conformational dynamics, while the experimental NMR results can inform calculations by defining site-specific preferred torsions of the dominant conformer and experimental conformer distributions, which may influence the initial REST-MD 3D geometry and the sampling ergodicity achieved, as reflected in the resultant histograms.

2 Results and Discussion

2.1 NAMFIS plus NMR line shape analysis

The ability of NMR to provide information on conformational dynamics, in addition to giving information on conformational preference, is useful in small molecule drug discovery. In Fig. 2a, each peak is doubled for compound **2** (1:1 ratio), instantly recognizable to NMR users as slow exchange of rotamers due to hindered bond rotation (measured half-life ~ 0.5 sec). As a guide to the eye, the signal(s) for the benzylic CH proton at ~ 5 ppm is/are highlighted in Fig. 2. The NMR spectrum reports two dominant conformers, equally populated, for the free ligand in solution for compound **2**. The bioactive conformation is one of a family of conformers (shown in green) with some flexibility around the pendant base. The alternative conformation (shown in orange) is the other, giving ~ 50% of the compound locked in a non-bioactive conformation. In contrast, Fig. 2b shows that compound **3** has a single set of sharp signals due to fast exchange (corresponds to a typical half-life of ~ nanoseconds, $\Delta v_{\frac{1}{2}}$ = 2.8 Hz). The ^{1}H NMR spectrum has a single isotropic chemical shift for both of the protons within one CH$_2$ functional group (these are not diastereotopic), an indication of local flexibility quickly picked up by an edited ^{13}C HSQC spectrum. Appreciation of the temporal dependence of free ligand exchange dynamics on NMR spectra can quickly inform medicinal chemists on local flexibility around bonds of newly synthesized molecules. This analysis, combined with potency data and matched molecular pair analysis, or a full comparison across a congeneric series, can provide critical insights into structure-activity relationships (Balazs et al., 2019).

Together with information regarding relative populations of conformations in solution, information about the magnitude of the rotational energy barrier between conformations, i.e. between one rotational isomer and another, is relevant information.

The challenge has been to get quick, easy, and comprehensive, yet accurate torsional profiles. Building a practicable and prospective visualization of conformational exchange dynamics around torsion angles into an NMR conformational analysis platform increases the potential to impact design, by highlighting the potential energy penalty of restricting torsions. To evaluate the dynamics, incorporating REST-MD into the workflow met the goal of expanding the current free ligand conformational analysis platform to make use of kinetic parameters from NMR spectra, e.g. signal line widths, while keeping within practical time limit constraints for Medicinal Chemistry design cycles.
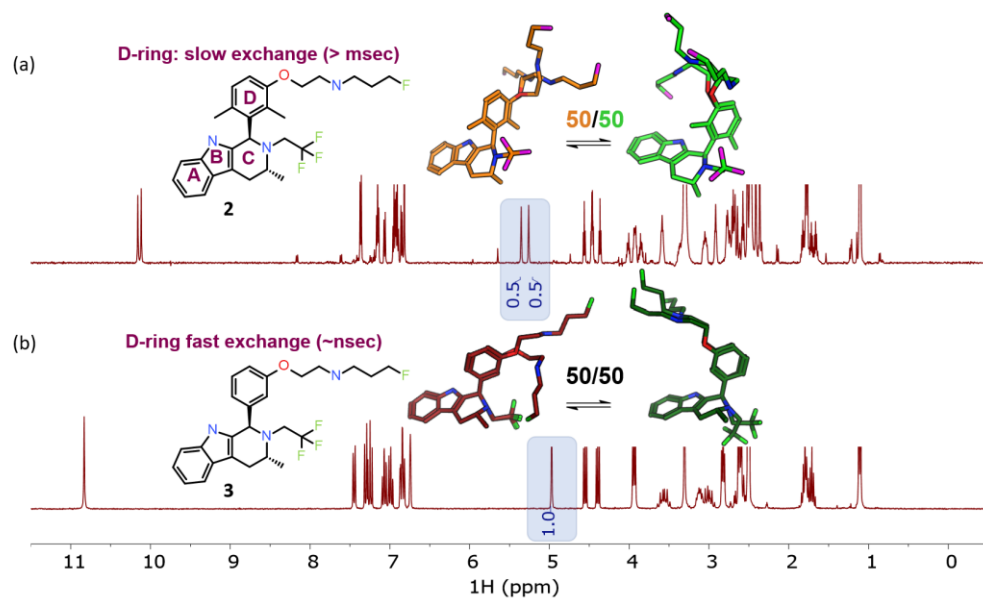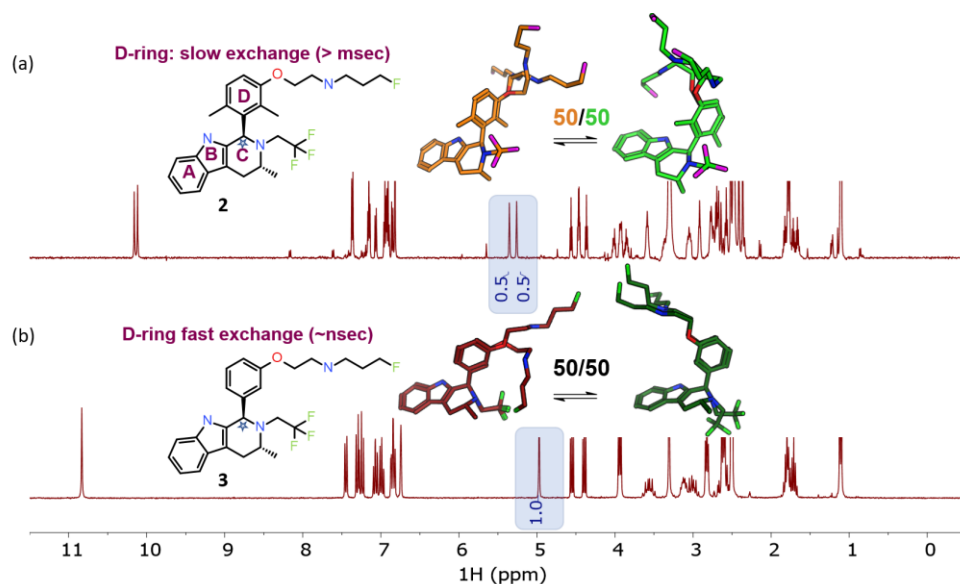
Figure 2 . NMR spectra inherently capture kinetic information from conformational dynamics (rotational energy barriers) in the signal line widths. The benzylic CH (the starred CH in ring 'C') is highlighted to exemplify the spectral changes between the dimethyl and des-methyl analogs. (a) The ^{1}H NMR spectrum shows rotamers with equal populations undergoing slow exchange on the NMR timescale. Profiling of 2 gave pIC$_{50}$ 8.9 and logD 4.8, with 50% bioactive conformation of the free ligand in DMSO-d_6 solution. (b) A spectrum with population weighted conformational averaging due to low barriers to rotation around bonds and fast exchange on the NMR timescale. Profiling of 3 resulted in pIC$_{50}$ 8.8, logD 4.1, 50% free ligand solution bioactive conformation. For this molecular matched pair we see similarities in the percent bioactive conformation in solution and the potency, regardless of the increased logD.

REST-MD predicts a comprehensive torsional profile in silico for rotatable bonds represented in a 2D molecular structure, while keeping computational speed and accuracy high. GPUs make REST-MD calculations feasible within drug discovery design cycle times. Ligand-based REST-MD simulates a ligand in explicit solvent at room temperature, allowing for conformational effects often neglected due to computational expense. The ligand conformers are sampled according to their Boltzmann populations and resultant reports visualize rotational torsion energies (Fig. 3). High accuracy fragment based calculations of rotational energy barriers (kcal/mol) are plotted as a function of bond torsion angle (solid lines). A superimposition of histograms counting the number of times the particular bond was observed at any particular angle is plotted onto the rotational energy barrier plot showing the torsion potential at each dihedral angle, summarizing the conformational space sampled during the REST-MD simulation. Such reports augment the ^{1}H NMR spectral interpretation, providing quantitative energy minima and theoretical distributions of conformers.
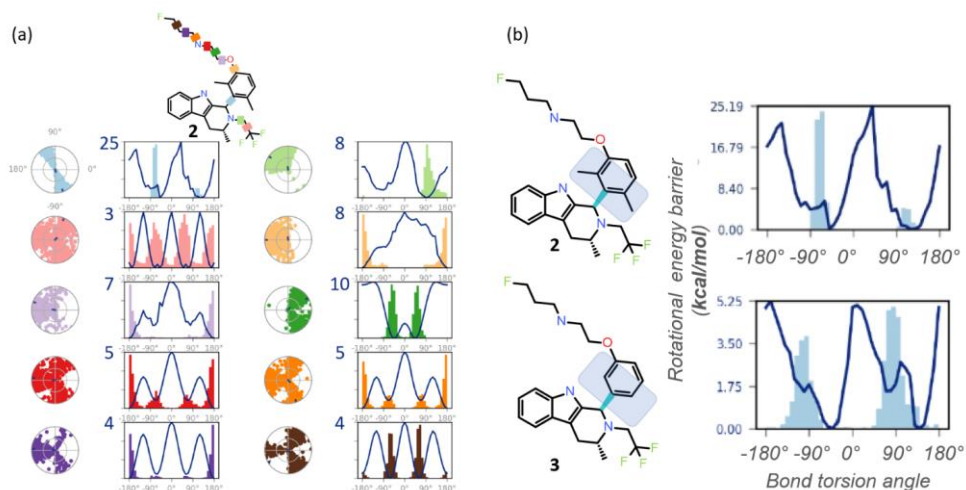
Figure 3. REST-MD visualizations, implemented in Maestro (Schrödinger, 2020b) complement atomic resolution NMR interpretations of structural dynamics across all bonds. (a) Simulation interaction diagrams report the rotational energy barrier (kcal/mol) as a function of the bond rotation angle. The conformational space sampled during the simulation is reported either as a function of the simulation time (radial plots, from the center at the start and spiraling outward) or as histograms superimposed on the torsion energy profiles (kcal/mol vs bond angle across each color coded bond in the molecule). Profiles are readily compared between molecular bonds that are pre-organized (light blue with y-axis maximum in the plot at 25 kcal/mol, with a bimodal radial plot and two energy minima), and flexible (pink with 3 kcal/mol maximum y-axis value, three energy minima, equally populated, and a randomly populated radial plot). (b) The barrier to rotation of the dimethyl is calculated to be, based on the lower of the two barriers, ~20 kcal/mol. Whereas experimentally both energy minima are equally populated as seen by the 1:1 ratio by NMR, the sampling conditions of the rigid "blue" bond were insufficient in the simulation to equally populate both wells. The NMR data in such cases clearly informs on the calculated predictions. A separate REST-MD simulation for the des-methyl compound, 3, was < 6 kcal/mol calculated rotational energy barrier for the same "blue" bond, consistent with sharp lines and ready conversions between the two conformers, with a broadened range of torsions, albeit still bimodal.

2.2 NMR measured rotational energy barrier

Methylation is a familiar and fundamental structural rigidification tool in a Medicinal Chemist's toolbox. In Fig. 2 methylation of the D ring demonstrates restricted bond rotation by the presence of rotameric signals in the ^{1}H NMR spectrum. Such restricted bond rotations, on millisecond timescales, occur when barriers to rotation about a bond are high (>~15 kcal/mol under ambient conditions). In contrast, a structural analog without methyl groups on the D ring displays free bond rotation on the NMR timescale (~ nanoseconds). Typically such barriers to rotation at room temperature correspond to ~ 5 kcal/mol (LaPlante et al., 2011a; LaPlante et al., 2011b; Wipf et al., 2015). The NMR spectrum of the ensemble of rapidly exchanging conformations reflects the Boltzmann weighted average of the chemical shifts, *J*-couplings, and interproton distances, with a single set of sharp peaks.

To locate the bond with the hindered rotation, chemical intuition is often sufficient. Using variable temperature NMR and/or exchange spectroscopy, the rotational energy barrier and the torsional rotation half-life of exchange can be determined. Fig. 4 shows ^{1}H NMR spectra as a function of eight different temperatures. The spectrum near room temperature has two equal

135 rotameric populations undergoing slow exchange on the NMR timescale, and highlighted in the figure. With increasing temperature the peaks coalesce and then begin to narrow. Increasing the temperature not only increases the rotation rate of the aromatic ring, it also increases the rate of fluctuations in the pendant base and the CH_2CF_3 groups and between axial *vs.* equatorial methyl orientation in ring C. Overall, this drives a shift to higher ppm for the exchange averaged signal with increasing temperature (Fig. 4).

Temp (K)	1/RT	k	ln(k)	$t_{\frac{1}{2}}$ (ms)
300	0.000401	0.0014	-6.5713	495
305	0.000394	0.0024	-6.0323	289
310	0.000388	0.0041	-5.4968	169

140
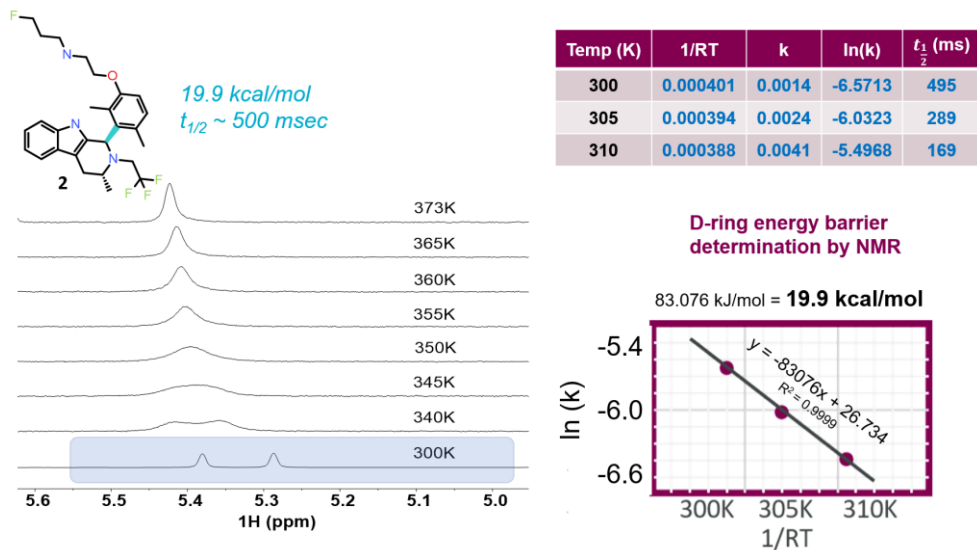
Figure 4. VT NMR stacked plots for the dimethyl compound undergoing slow to fast exchange with increasing temperature. To measure the energy barrier to rotation of the D-ring, three temperatures and a 1D selective EXSY at different mixing times was used to estimate the exchange rates and half-life. An Arrhenius plot gives the barrier to rotation at 19.9 kcal/mol and the 300 K half-life is ~ 0.5 sec.

145 In order to determine the barrier to rotation around the aromatic ring, it was important to collect data within a temperature range where exchange rates were dominated by the dynamics of interest in order to follow a simple two-state model for analysis. Therefore, three temperatures at 300, 305, and 310 K were chosen and exchange spectroscopy was performed with selective inversion on the peak near 5.3 ppm. At each of the three temperatures 8 mixing times (100, 200, 300, 400, 500, 700, 1000, and 2000 milliseconds) were used to determine the first order rate kinetics, with the fitted value for k given in

150   tabular form in Fig. 4. The half-life was derived from ln(2)/k. The fitted plot of ln(k) vs. 1/RT is shown, revealing a value of 19.9 kcal/mol for the barrier to rotation.

2.3 NMR informs calculations

    REST-MD generates a large ensemble of (~1000) conformations, in explicit solvent. REST-MD was run with Desmond (Schrödinger, 2020a) with the pendant base initially oriented either forward or backward relative to the tricyclic core for **1**.

155   The resultant calculated energy barrier of ~ 20 kcal/mol (Fig. 3b) is in agreement with the NMR determined value of 19.9 kcal/mol. The REST-MD visualization confirmed chemical intuition that the source of the rotameric species is the bond between the tricyclic core and the aromatic ring. Advantageously, the full torsional profile report from the REST-MD simulation can be run prospectively to rank design ideas, for instance to test a hypothesis around rigidification and the degree of bioactive pre-organization induced. The ability of REST-MD to evaluate torsion angles prior to synthesis can also flag

160   chemists to check the NMR for site-specific dynamics information at the time of structural verification. Such information could alert the team to add a diagnostic selective-NOE measurement to the standard acquisition suite, to test a free ligand conformational hypothesis post synthesis, while the solution sample is in the spectrometer for structural identification. Conversely, the NMR can supply experimental details inaccessible to the calculations, particularly helpful within a chemical series, as the lessons are generally translatable across the structural analogs. For instance, the ^{1}H NMR spectrum of the

165   dimethyl compound **2** showed a 1:1 ratio between the two exchanging conformations (Fig. 2). Whereas REST-MD conformational sampling shows only one of the two minima populated (Fig. 5). The fragment based energy calculation, shown as a solid line in the REST-MD torsional profiles, is consistently the same, even using a very short simulation time (e.g. picoseconds). The histograms vary based on initial conformation and number of replicates run. Starting with an initial conformation with the pendant base facing "forward" relative to the tricyclic core, the radial plot of torsion angle

170   representation as a function of time starting at the center and spiraling outward, only populates the ~ +90° bond torsion angle during the 50 ns simulation that has a temperature range of 300 - 1263 K (12 replicates, 50 nanoseconds). Analogously, the histogram has one energy minimum populated and the number of times the ~ +90° torsion was observed is fairly narrowly distributed (Fig. 5, top). With the same initial conformation, increasing the temperature range to a high of 3302 K (20 replicates, 50 nanoseconds), showed some evidence of sampling of the opposite conformation in the radial plot (Fig. 5,

175   middle). Starting the simulation with the 3D conformation switched to put the pendant base towards the back instead and running 20 replicates for a higher sampling temperature shows both minima were sampled (Fig. 5, bottom). Once this compound has been synthesized, it then becomes experimentally apparent from the 1H NMR spectrum at 300 K in DMSO-d_6 that both minima are equally populated (Fig. 2a). In this manner the experimental results can be fed-back to the calculations to refine details and gauge areas of caution during interpretation.

	"backward"	"forward"	Replicates	Temperature range Max (K)
			12	1263
			20	3302
			20	3302

180
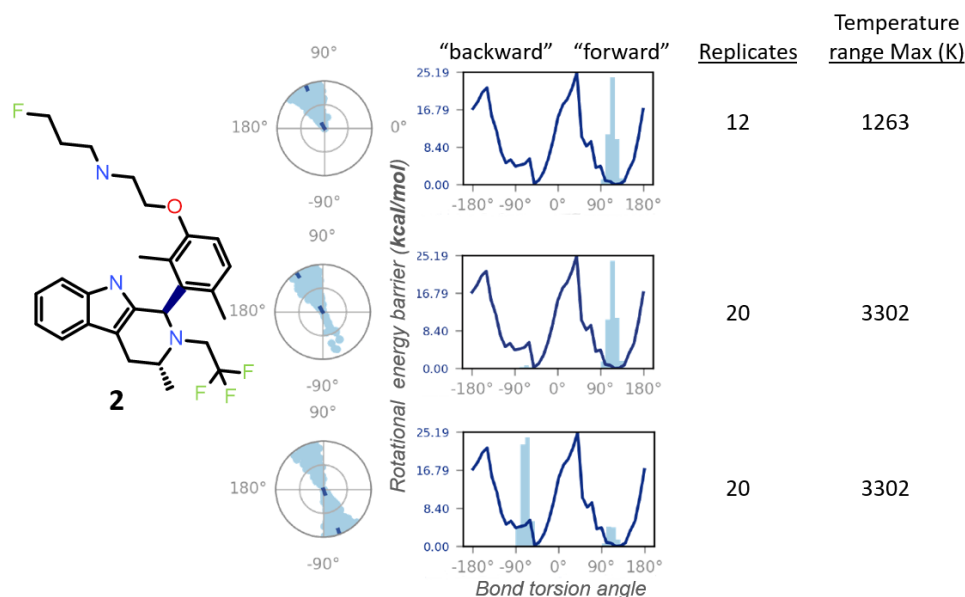
Figure 5. The REST-MD simulation of the dimethyl compound 2 predicts a preference to populate only one energy minimum, correlated with the initial dihedral angle starting condition in the simulation. Shown are results from calculations for conformations sampled as a function of bond rotation angle for the bond between the tricyclic core and the aromatic ring, bolded in the molecular structure. The three different simulation conditions are, from top to bottom: starting with the pendant base facing forward (~ +90º) with a temperature range of 300 - 1263 K (12 replicates); same initial conformation, with a temperature range of 300 - 3302 K (20 replicates); and the opposite initial conformation, with the pendant base facing backward, run with 20 replicates (300 - 3302 K). All REST-MD simulations ran for 50 nanoseconds.

2.4 REST-MD/NMR synergy in drug discovery

What REST-MD adds to the existing NMR platform is visualization of conformational dynamics, by providing calculated rotational energy barriers across all bonds. This complements NMR spectral data to give insight into flexibility / rigidity at atomic resolution. Together, REST-MD and NMR conformational analysis allows us to utilize all the spectral information, thermodynamic and kinetic, gathered from ^{1}H NMR spectra: chemical shifts, J-couplings, NOEs and linewidths, to maximize characterization of free ligands in solution.

Without REST-MD, NMR alone can provide valuable information on the experimental conformational preference of the free ligand in solution. From the NMR alone, the relative populations of each conformer in solution can be deduced. And it can be determined if the dominant conformer in solution is pre-organized into the bioactive conformation, which is of practical value for drug discovery. However, adding REST-MD provides an easy and practical way to visualize the magnitude of the

energy penalty paid if the bioactive conformation is not highly populated in solution. This can help rationalize the cost to benefit ratio of ~~effort invested in designing an increase in the percent bioactive conformation by restricting rotation~~ design
team effort invested in increasing the percentage of free ligand pre-organized into a bioactive conformation. As drug discovery requires optimization of several parameters, knowing when binding has been optimized can shift design focus and resources towards improving physicochemical properties.

The added benefit of REST-MD is its ability to deliver prospective information regarding structural ideas of compounds, not yet synthesized. Accurate predictions of free ligand solution conformational dynamics can help rank compounds to focus synthesis prioritization and flag supplemental experiments, such as selective NOEs on atom pairs to quickly ascertain expected conformations.

While the full torsional profile is powerful on its own, the REST-MD results also provide an extensively sampled conformational ensemble in explicit solvent that can be clustered and fed forward for use in NMR conformational analysis. Taking the selected conformer set forward for QM geometry refinements and calculations of NMR chemical shift and coupling constants provides the modeled parameter set used for further NAMFIS based analysis. Using the conformer set generated by REST-MD is particularly helpful for higher molecular weight small molecules which begin to self-associate~~d~~ during low mode MD conformational searches (LaBute, 2010) using a polarizable continuum model to emulate solvent~~,~~. Low mode MD provides a comprehensive search of the conformational ensemble, but can therefore result~~ing~~ in a set highly biased towards collapsed conformations.

3 Methods

3.1 NMR Spectroscopy

^{1}H NMR spectra were recorded at 300 K on a 500 MHz NEO or a 600 MHz AVIII Bruker spectrometer with TCI cryoprobes. Solutions were made from 1-4 mg solid freshly dissolved in DMSO-d_6. Spectra were acquired with a 30 degree hard pulse, a 1 sec delay, 2 dummy shots, and signal averaged over 16 transients. A spectral width of ~ 20 ppm with 64k points was used. Spectral analysis was performed using Advanced Chemistry Development, Inc. (ACD/Labs) Spectrus Processor (ACD/Labs, Version 2020.1.2). 2D ROESY was run with the Bruker standard pulse program roesyadjsphpr with ns 4, TD (1024, 256), and a 200 ms spin-lock.

3.1.1 Compound 1

^{1}H NMR (500 MHz, DMSO-d_6) Shift 10.54 (s, 1H), 7.44 (d, J = 7.7 Hz, 1H), 7.23 (d, J = 8.0 Hz, 1H), 7.03 (td, J = 7.9, 1.2 Hz, 1H), 6.99 (t, J = 8.2 Hz, 1H), 6.97 (td, J = 8.0, 1.2 Hz, 1H), 6.89 (d, J = 7.9 Hz, 1H), 6.28 (br d, J = 8.2 Hz, 1H), 5.14 (s, 1H), 4.51 (dt, J = 47.5, 6.1 Hz, 2H), 4.00 (t, J = 5.6 Hz, 2H), 3.46 (dq, J = 16.0, 10.6 Hz, 1H), 3.37 – 3.33 (m, 1H), 2.99 (dq, J = 16.0, 10.0 Hz, 1H), 2.90 (t, J = 5.7 Hz, 2H), 2.78 (dd, J = 16.0, 4.5 Hz, 1H), 2.69 (t, J = 6.9 Hz, 2H), 2.62 (dd, J = 16.0, 7.7 Hz, 1H), 2.53 – 2.51 (m, 1H), 2.28 (s, 3H), 1.85 – 1.74 (m, 2H), 1.06 (d, J = 6.7 Hz, 3H)

3.1.2 Compound 2

[230] ^{1}H NMR (500 MHz, DMSO-d_6) Shift 10.18 (s, 0.5H, isomer1), 10.14 (s, 0.5H, isomer2), 7.39 (d, J = 7.6 Hz, 1H, isomer1+isomer2), 7.18 (t, J = 7.2 Hz, 1H, isomer1+isomer2), 7.09 (d, J = 8.5 Hz, 0.5H, isomer2), 6.99 – 6.95 (m, 1H, isomer1+isomer2), 6.95 – 6.90 (m, 1H, isomer1+isomer2), 6.88 (d, J = 8.4 Hz, 0.5H, isomer2), 6.84 (s, 1H, isomer1), 5.38 (s, 0.5H, isomer1), 5.29 (s, 0.5H, isomer2), 4.54 (dt, J = 47.5, 6.0 Hz, 1H, isomer1), 4.44 (dt, J = 47.5, 6.0 Hz, 1H, isomer2), 4.07 – 3.95 (m, 1H, isomer1), 3.95 – 3.85 (m, 1H, isomer2), 3.67 – 3.56 (m, 1H, isomer1+isomer2), 3.39 (s, 1H, [235] isomer1+isomer2), 3.14 – 3.04 (m, 1H, isomer1+isomer2), 2.94 (br t, J = 5.4 Hz, 1H, isomer1), 2.80 (br t, J = 5.6 Hz, 1H, isomer2), 2.77 (br d, J = 4.5 Hz, 1H, isomer1+isomer2), 2.72 (t, J = 7.0 Hz, 1H, isomer1), 2.69 (br d, J = 15.0 Hz, 1H, isomer1+isomer2), 2.60 (t, J = 6.9 Hz, 1H, isomer1+isomer2), 2.44 (s, 1.5H, isomer2), 2.39 (s, 1.5H, isomer1), 1.83 (br dquin, J = 26.2, 6.6 Hz, 1H, isomer1), 1.82 (s, 1.5H, isomer2), 1.80 (s, 1.5H, isomer1), 1.72 (dquin, J = 26.2, 6.4 Hz, 1H, isomer2), 1.14 (d, J = 6.5 Hz, 3H, isomer1+isomer2)

[240] ### 3.1.3 Compound 3

^{1}H NMR (600 MHz, DMSO-d_6) Shift 10.86 (s, 1H), 7.45 (d, J = 7.8 Hz, 1H), 7.31 (d, J = 8.0 Hz, 1H), 7.26 (t, J = 7.8 Hz, 1H), 7.08 (dd, J = 8.0, 7.5 Hz, 1H), 7.00 (dd, J = 7.8, 7.5 Hz, 1H), 6.86 (dd, J = 8.2, 2.4 Hz, 1H), 6.84 (d, J = 7.8 Hz, 1H), 6.75 (br d, J = 2.3 Hz, 1H), 4.98 (s, 1H), 4.48 (dt, J = 47.5, 6.6 Hz, 2H), 3.95 (t, J = 5.6 Hz, 2H), 3.57 (qd, J = 13.0, 9.3 Hz, 1H), 3.12 (dqd, J = 11.0, 6.8, 5.0 Hz, 1H), 3.01 (qd, J = 18.0, 9.3 Hz, 1H), 2.83 (t, J = 5.7 Hz, 2H), 2.64 (dd, J = 15.8, 5.0 Hz, [245] 1H), 2.57 (dd, J = 15.8, 11.0 Hz, 1H), 2.62 (t, J = 6.6 Hz, 2H), 1.76 (dquin, J = 26.1, 6.6 Hz, 2H), 1.11 (d, J = 6.8 Hz, 3H)

3.2 Exchange Spectroscopy

^{1}H NMR spectra were recorded on a 500 MHz NEO at 300, 305, 310, 340, 345, 350, 355, 360, 365, and 373 K. For the 1D selective exchange spectroscopy at 300, 300, and 310 K, the mixing times used were 100, 200, 300, 400, 500, 700, 1000, and 2000 milliseconds. The spectra were integrated with consistent integral ranges and calibrating the integral of the inverted [250] peak to 100 to consistently normalize the data (Hu and Krishnamurthy, 2006). An excel spreadsheet was used to calculate the fractional intensity increase as a function of mixing time to fit exchange rate and half-life (Bovey, 1988; Li, et al., 2007).

3.3 REST-MD

Two different initial molecular conformations were run where the variation was place on the relative position of the pendant base to the tricyclic ring: (i) "forward" or (ii) "backward", using the same atom numbering for all conformations sampled for [255] the same compound, to simplify later steps in the workflow. Molecular protonation states at pH 7.0 ± 0.0 were used for the MD simulations. The force field builder in Maestro (Schrödinger, 2020b) was used to customize the OPLS3e force field for the system builder where a NaCl salt concentration of 0.15 M was used and the base was neutralized by addition of 1 Na+ ion during creation of the explicit water shell for solvation using the predefined SPC model and an orthorhombic box shape

of 10 Å x 10 Å x 10 Å using the "buffer" box size calculation method. Desmond (Schrödinger, 2020a) replica exchange with solute tempering molecular dynamics was run with 12 replicas giving a temperature range of 300 K to typically ~1300 K, for a total of 50 ns for extensive sampling of conformational space during the simulation.

3.4 Simulation Interaction Diagram

The plots automatically generated in Maestro (Schrödinger, 2020b) provide solid lines tracing out the barrier to rotation in kcal/mol as a function of the torsion angle. The histograms provide the resulting distribution of 1002 conformers under our routine sampling conditions. Radial plots show the evolution of the simulation time from the start, at the center.

3.5 Clustering of Conformers

Ligands, without the solvent shell, were extracted from the REST-MD trajectories for both sets of initial conformers (forward and backward). To aid a quick visual inspection of the results, conformers was superimposed using the SMARTS method and the substructure smiles string of c12c(C)c(CN)[nH]c1cccc2 to align the conformers relative to the rigid tricyclic ring. Conformers were clustered in Maestro (Schrödinger, 2020b) by atomic RMSD, discarding mirror-image conformers, selecting the option of one structure (nearest to centroid) per cluster, thus reducing the full set down to representative diverse conformers, typically 15 - 40.

3.6 QM Calculations

Chemical Computing Group's (Molecular Operating Environment (MOE), 2019.01) conformational search GUI was employed to generate input files for Gaussian 16 (Revision C.01) after importing conformers into a molecular database and using the wash function to neutralize charged species not observed by NMR in DMSO-d_6 solutions. QM geometry refinement, chemical shift calculations and coupling constant calculations were carried out with the GIAO DFT method at the B3LYP/6-31G* level with PCM solvent modeling using a dielectric constant of 78.4. Geometry optimization keywords were set with opt=(tight,RecalcFC=5,MaxCycles=5000) and Int=SuperFineGrid.

3.7 Conformer Distribution

MOE's Spectral Analysis GUI was employed for least squares fits of chemical shifts to determine conformer distributions; the option for couplings and NOE's was used selectively.

4 Conclusions

The REST-MD protocols described above provide rapid and prospective access to torsional energy barriers and conformational states for drug-like molecules. The REST-MD calculations accurately reproduce and visualize NMR dynamics which synergistically work with experimental conformational exchange dynamics obtained from 1D ^{1}H NMR

spectra. Integration of REST-MD into our NMR conformational analysis platform has enabled visualization of atomic level information by all medicinal chemists and can be readily used to guide design hypotheses toward molecules with improved potency and or physicochemical properties.

290   This new methodology has been applied across more than 10 early oncology projects in 2020, both small molecules and PROTACs, to answer questions around conformational preference (populations) and dynamics (rotational barriers).

In addition, NMR provides design teams with information on the presence of intramolecular hydrogen bonds (IMHB), and the combined influences on properties such as potency, permeability and oral bioavailability. Diverse applications have enabled refinement of the approach, and represents a step towards the goal of routine use for prospective design and

295   determination of experimentally based conformation-activity relationships.

Author contribution

AB and EC drove the earliest drafts of this manuscript, to which all authors have contributed. MP developed and optimized computational workflows. DL and ND determined the energy barrier to rotation by NMR. AB ran REST-MD simulations in Schrödinger and NAMFIS-based analyses in MOE. All authors contributed valuable discussions to the preparation of this

300   manuscript.

Competing interests

All authors are shareholders in AstraZeneca PLC.

Acknowledgements

The entire SERD team, including the analytical, computational, synthetic, and lead chemists, from the extended Oncology

305   R&D group are gratefully acknowledged for chemical designs, syntheses, purifications and compound profiling. We thank Jason Breed for the crystallography providing protein-ligand and bound conformations shown in Figure 1. An excel spreadsheet with detailed methodology for the 1D selective EXSY was kindly provided by David Whittaker. We thank Jamie Scott and Michelle Lamb for valuable feedback on the manuscript.

References

310   ACD/ChemSketch,   version   2020.1.2,   Advanced   Chemistry   Development,   Inc.,   Toronto,   ON,   Canada, http://www.acdlabs.com, 2021.

Atilaw, Y., Poongavanam, V., Nilsson, C. S., Nguyen, D., Giese, A., Meibom, D., Erdelyi, M., and Kihlberg, J.: Solution Conformations Shed Light on PROTAC Cell Permeability, ACS Med. Chem. Lett., 12, 107-114, https://doi.org/10.1021/acsmedchemlett.0c00556, 2021.

Balazs, A. Y. S., Carbajo, R. J., Davies, N. L., Dong, Y., Hird, A. W., Johannes, J. W., Lamb, M. L., McCoull, W., Raubo, P., Robb, G. R., Packer, M. J., and Chiarparin, E.: Free Ligand 1D NMR Conformational Signatures To Enhance Structure Based Drug Design of a Mcl-1 Inhibitor (AZD5991) and Other Synthetic Macrocycles, Journal of medicinal chemistry, 62, 9418-9437, doi:10.1021/acs.jmedchem.9b00716, 2019.

Blundell, C. D., Nowak, T., and Watson, M. J.: Measurement, Interpretation and Use of Free Ligand Solution Conformations in Drug Discovery, Progr. Med. Chem., 55, 45-147, https://doi.org/10.1016/bs.pmch.2015.10.003, 2016.

Blundell, C., Packer, M., and Almond, A.: Quantification of free ligand conformational preferences by NMR and their relationship to the bioactive conformation, Bioorganic & medicinal chemistry, 21, 4976-4987, doi:10.1016/j.bmc.2013.06.056, 2013.

Bovey, F. A.: Nuclear Magnetic Resonance Spectroscopy, Second Edition, Academic Press, Inc., San Diego, California, pp. 291-299, https://doi.org/10.1016/B978-0-08-091699-6.50010-6, 1988.

Chiarparin, E., Packer, M. J., and Wilson, D. M.: Experimental free ligand conformations: a missing link in structure-based drug discovery, Future Med. Chem., 11, 79-82, https://doi.org/10.4155/fmc-2018-0339, 2019.

Cicero, D., Barbato, G., and Bazzo, R.: NMR Analysis of Molecular Flexibility in Solution: A New Method for the Study of Complex Distributions of Rapidly Exchanging Conformations. Application to a 13-Residue Peptide with an 8-Residue Loop, J. Am. Chem. Soc., 117, 1027-1033, https://doi.org/10.1021/ja00108a019, 1995.

de Sena M Pinheiro, P., Rodrigues, D. A., do Couto Maia, R., Thota, S., and Fraga, C.: The Use of Conformational Restriction in Medicinal Chemistry, Curr. Top. Med. Chem., 19, 1712-1733, https://doi.org/10.2174/1568026619666190712205025, 2019.

Fang, Z., Song, Y., Zhan, P., Zhang, Q., and Liu, X.: Conformational restriction: an effective tactic in 'follow-on'-based drug discovery, Future Med. Chem., 6, 885-901, https://doi.org/10.4155/fmc.14.50, 2014.

Farès, C., Lingnau, J. B., Wirtz, C., and Sternberg, U., Conformational Investigations in Flexible Molecules Using Orientational NMR Constraints in Combination with ^{3}*J*-Couplings and NOE Distances. Molecules, 24, 4417-4441. https://doi.org/10.3390/molecules24234417, 2019.

350 Foloppe, N. and Chen, I.-J.: Towards understanding the unbound state of drug compounds: Implications for the intramolecular reorganization energy upon binding, Bioorgan. Med. Chem., 24, 2159-2189, https://doi.org/10.1016/j.bmc.2016.03.022, 2016.

Gaussian 16, Revision C.01, Frisch, M. J., Trucks, G. W., Schlegel, H. B., Scuseria, G. E., Robb, M. A., Cheeseman, J. R.,
355 Scalmani, G., Barone, V., Petersson, G. A., Nakatsuji, H., Li, X., Caricato, M., Marenich, A. V., Bloino, J., Janesko, B. G., Gomperts, R., Mennucci, B., Hratchian, H. P., Ortiz, J. V., Izmaylov, A. F., Sonnenberg, J. L., Williams-Young, D., Ding, F., Lipparini, F., Egidi, F., Goings, J., Peng, B., Petrone, A., Henderson, T., Ranasinghe, D., Zakrzewski, V. G., Gao, J., Rega, N., Zheng, G., Liang, W., Hada, M., Ehara, M., Toyota, K., Fukuda, R., Hasegawa, J., Ishida, M., Nakajima, T., Honda, Y., Kitao, O., Nakai, H., Vreven, T., Throssell, K., Montgomery, J. A., Jr., Peralta, J. E., Ogliaro, F., Bearpark, M. J.,
360 Heyd, J. J., Brothers, E. N., Kudin, K. N., Staroverov, V. N., Keith, T. A., Kobayashi, R., Normand, J., Raghavachari, K., Rendell, A. P., Burant, J. C., Iyengar, S. S., Tomasi, J., Cossi, M., Millam, J. M., Klene, M., Adamo, C., Cammi, R., Ochterski, J. W., Martin, R. L., Morokuma, K., Farkas, O., Foresman, J. B., Fox, D. J. Gaussian, Inc., Wallingford CT, 2016

Hu, H. and Krishnamurthy, K.: Revisiting the initial rate approximation in kinetic NOE measurements, J. Magn. Reson.,
365 182, 173-177, https://doi.org/10.1016/j.jmr.2006.06.009, 2006.

Huang, X., Hagen, M., Kim, B., Friesner, R. A., Zhou, R., and Berne, B. J.: Replica exchange with solute tempering: efficiency in large scale systems, J. Phys. Chem. B, 111, 5405-5410, https://doi.org/10.1021/jp068826w, 2007.

370 Labute, P..: LowModeMD-Implicit Low-Mode Velocity Filtering Applied to Conformational Search of Macrocycles and Protein Loops, J. Chem. Inf. Model., 50, 792-800, https://doi.org/10.1021/ci900508k, 2010.

LaPlante, S. R., Edwards, P. J., Fader, L., Jakalian, A., and Hucke, O.: Revealing atropisomer axial chirality in drug discovery, ChemMedChem, 6, 505-513 https://doi.org/10.1002/cmdc.201000485, 2011a.
375
LaPlante, S. R., Fader, L. D., Fandrick, K. R., Fandrick, D. R., Hucke, O., Kemper, R., Miller, S. P. F., and Edwards, P. J.: Assessing atropisomer axial chirality in drug discovery and development, J. Med. Chem., 54, 7005-7022, https://doi.org/10.1021/jm200584g, 2011b.

380   LaPlante, S. R., Nar, H., Lemke, C. T., Jakalian, A., Aubry, N., and Kawai, S. H.: Ligand bioactive conformation plays a critical role in the design of drugs that target the hepatitis C virus NS3 protease, J. Med. Chem., 57, 1777-1789, https://doi.org/10.1021/jm401338c, 2014.

Li, F., Zhang, H., Jiang, L., Zhang, W., Nie, J., Feng, Y., Yang, M., and Liu, M.: Dynamic NMR study and theoretical
385   calculations on the conformational exchange of valsartan and related compounds, Magn. Reson. Chem., 45, 929-936, https://doi.org/10.1002/mrc.2072, 2007.

Liu, P., Kim, B., Friesner, R A.., and Berne, B. J.: Replica exchange with solute tempering: a method for sampling biological systems in explicit water, P. Natl. Acad. Sci. USA, 102, 13749-13754, https://doi.org/10.1073/pnas.0506346102, 2005.
390

Molecular Operating Environment (MOE), 2019.01, Chemical Computing Group ULC, 1010 Sherbooke St. West, Suite #910, Montreal, QC, Canada, H3A 2R7, 2021.

Nevins, N., Cicero, D., and Snyder, J. P.: A Test of the Single-Conformation Hypothesis in the Analysis of NMR Data for
395   Small Polar Molecules: A Force Field Comparison, J. Org. Chem., 64, 3979-3986, https://doi.org/10.1021/jo9824450, 1999.

Schrödinger Release 2020-3: Desmond Molecular Dynamics System, D. E. Shaw Research, New York, NY, 2020. Maestro-Desmond Interoperability Tools, Schrödinger, New York, NY, https://www.schrodinger.com/products/desmond, 2020a.

400   Schrödinger Release 2020-3: Maestro, Schrödinger, LLC, New York, NY, https://www.schrodinger.com/products/maestro, 2020b.

Scott, J. S., Bailey, A., Davies, R. D., Degorce, S. L., MacFaul, P. A., Gingell, H., Moss, T., Norman, R. A., Pink, J. H., Rabow, A. A., Roberts, B., and Smith, P. D.: Tetrahydroisoquinoline Phenols: Selective Estrogen Receptor Downregulator
405   Antagonists with Oral Bioavailability in Rat, ACS Med. Chem. Lett., 7, 94-99, https://doi.org/10.1021/acsmedchemlett.5b00413, 2016.

Scott, J. S., Bailey, A., Buttar, D., Carbajo, R. J., Curwen, J., Davey, P. R. J., Davies, R. D. M., Degorce, S. L., Donald, C., Gangl, E., Greenwood, R., Groombridge, S. D., Johnson, T., Lamont, S., Lawson, M., Lister, A., Morrow, C. J., Moss, T. A.,
410   Pink, J. H., and Polanski, R.: Tricyclic Indazoles-A Novel Class of Selective Estrogen Receptor Degrader Antagonists, J. Med. Chem., 62, 1593-1608, https://doi.org/10.1021/acs.jmedchem.8b01837, 2019.

Scott, J. S., Moss, T. A., Balazs, A, Barlaam, B, Breed, J, Carbajo, R. J., Chiarparin, E., Davey, P. R. J., Delpuech, O., Fawell, S., Fisher, D. I. Gagrica, S., Gangl, E. T., Grebe, T., Greenwood, R. D,. Hande, S., Hatoum-Mokdad, H., Herlihy, K., Hughes, S., Hunt, T. A., Huynh, H., Janbon, S. L. M., Johnson, T., Kavanagh, S., Klinowska, T., Lawson, M., Lister, A. S., Marden, S., McGinnity, D. F,. Morrow, C. J., Nissink J. W. M., O'Donovan, D. H., Peng, B., Polanski, R., Stead, D. S., Stokes, S, Thakur, K., Throner, S.R., Tucker, M. J., Varnes, J., Wang, H., Wilson, D. M., Wu, D., Wu, Y., Yang, B., and Yang, W.: Discovery of AZD9833, a Potent and Orally Bioavailable Selective Estrogen Receptor Degrader and Antagonist, 63, 14530-14559, J. Med. Chem., https://doi.org/10.1021/acs.jmedchem.0c01163, 2020.

Slabber, C. A., Grimmer, C. D., and Robinson, R. S.: Solution Conformations of Curcumin in DMSO, J. Nat. Prod., 79, 2726-2730, https://doi.org/10.1021/acs.jnatprod.6b00726, 2016.

Wang, L., Friesner, R. A., and Berne, B. J.: Replica exchange with solute scaling: a more efficient version of replica exchange with solute tempering (REST2), J. Phys. Chem. B, 115, 9431-9438, https://doi.org/10.1021/jp204407d, 2011.

Wipf, P., Skoda, E. M., and Mann, A.: Conformational Restriction and Steric Hindrance in Medicinal Chemistry, in: The Practice of Medicinal Chemistry, Fourth edition, edited by: Wermuth, C. G., Aldous, D., Raboisson, P., and Rognan, D., Academic Press, San Diego, 279 - 299, https://doi.org/10.1016/B978-0-12-417205-0.00011-0, 2015.

Wu, J., Lorenzo, P., Zhong, S., Ali, M., Butts, C. P., Myers, E. L., and Aggarwal, V. K.: Synergy of synthesis, computation and NMR reveals correct baulamycin structures, Nature, 547, https://doi.org/10.1038/nature23265, 2017.

Zondlo, N. J.: SAR by 1D NMR, J. Med. Chem., 62, 9415-9417, https://doi.org/10.1021/acs.jmedchem.9b01688, 2019.